IAC-19-C1.4.6

CONTRIBUTIONS OF VENUS SWING-BY MANEUVER IN EARTH-MARS TRANSFERS

Maisa O. Terra
Instituto Tecnológico de Aeronáutica, Brazil, maisa@ita.br

Antonio F. B. A. Prado
Instituto Nacional de Pesquisas Espaciais, Brazil, prado@dem.inpe.br

In this paper we investigate the role played by Jupiter in Earth-Mars transfers with a Venus flyby. For that, transfers are computed exploring the natural dynamics of the Restricted Three-Body Problem framework under the influence of the Sun and Jupiter gravitational potentials. The motivation for the gravity assist by Venus is two-fold. First, to design a mission to obtain data both from Venus and Mars, and second, to seek interesting solutions for a one-way or a round trip to Mars, providing a more flexible time window for a eventual return to the Earth. For the sake of comparison, direct Earth-Mars transfers are also built in the same framework. In both analysis, four parameters at departure of Earth are defined, while a fifth parameter appears in the transfers with the swing-by maneuver by Venus. We present our results and explore the effect of Jupiter in the trade-off between the Earth-Mars cost and the total Earth-Mars flight time. Additionally solutions with reduced waiting time for Hohmann transfer return to the Earth with higher values of total Δv are reported. We conclude suggesting possible applications and extensions of this preliminary analysis.

1. Introduction

Exploration and colonization of Mars, one of most prevalent themes in science fiction, have become a concrete goal by space agencies and aerospace engineering and scientific communities with the recent technology advances.

Among many technical aspects, interplanetary transfer design is challenging given the high complexity involving many-body effects, primaries orbit geometry, elevated cost, suitable time window for departure and return, and transfer time, among other issues. In particular, design of round-trip Earth Mars transfers must consider different approaches and strategies to provide solutions with diverse features for distinct mission proposals and capabilities.

The more efficient classical interplanetary solution is given by the Hohmann transfer. In this two-body formulation, planets are assumed to move on coplanar circular orbits and just the gravitational potential of the Sun defines the dynamics of the spacecraft. As a result, a trip from Earth to Mars takes about 258.8 days and requires a velocity variation of 5.59 km/s. For a round trip these quantities double, but a minimum waiting time of 453.8 days in Mars is required, adding up to a total of 971 days for a complete round trip mission. This total time can be shortened at the expense of additional cost and a large diversity of solutions may be obtained by patched conics approach as well. Additionally, Gravity assist maneuvers has also been exploited by many authors to get flexible mission time and profiles [1, 2, 3].

Ren et al. [4] recently explored fast and short-term mechanisms of natural transport in the Solar System. In particular, short-time interplanetary transport based on the exploitation of hyperbolic invariant manifolds associated to the collinear equilibria of the Restricted Three-Body Problem (R3BP) requires additional costs, given that pseudo-heteroclinic connections are not available, except for a few cases, such as, Jupiter-Saturn and Uranus-Neptune systems. Given that, many contributions have explored distinct strategies and techniques in the context of three-body formulations to seek suitable Earth-Mars transfer solutions with affordable costs and reasonable time [5, 6, 7].

In this paper, Earth-Mars transfers are investigated in the framework of the Planar Circular R3BP of the Sun-Jupiter system, considering a gravity assist maneuver by Venus. The direct Earth-Mars transfer is also considered for the sake of comparison. Besides, the possibility of data acquisition, the passage by Venus aims to provide a more flexible time for a return trip to the Earth.

The paper is organized as follows: In Section 2 some important key points are discussed, justifying the choice of the mathematical models and the strategy design. Section 3 introduces the numerical procedure to design Earth-Mars transfer with and without a Venus Swing-by.

Section 4 presents and discusses the obtained results for the direct transfers and for the transfers with a Venus close approach. Finally, final remarks and perspective of future works are presented in Section 5.

2. Brief discussion of important key points

In this section, some important key points are addressed, aiming to clarify the choices undertaken in this investigation.

2.1 The choice of the Sun-Jupiter system

Besides the Sun, in the vicinity of the interplanetary region between the orbits of Earth and Mars, the dominant forces are given by the gravity of the Earth, Mars and Jupiter, as shown by Fig. 5 of Ref. [4]. For this reason, as an effort to include many-body effects in the interplanetary phase of the Earth-Mars transfer design, we consider the Circular Restricted Three-Body Problem with the Sun and Jupiter as the primary bodies P_1 and P_2. For simplicity, in a preliminary analysis, we assume that motion of the planets are given by coplanar circular orbits, as illustrated by Fig. 1, that shows a schematic representation of the main elements of the transfer in the heliocentric inertial frame (namely, the primaries Sun (S) and Jupiter (J), and the orbits of Earth, Mars and Venus).

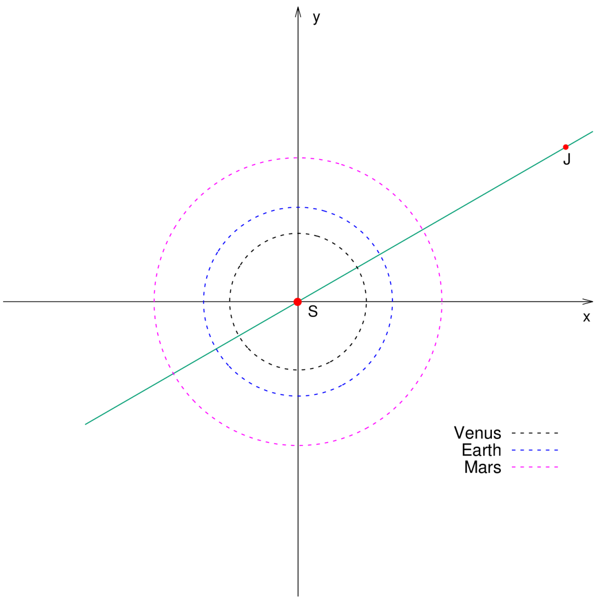

Figure 1: Schematic representation of the main elements of the transfer in the heliocentric inertial frame, namely, the primaries Sun (S) and Jupiter (J), and the orbits of the planets Earth, Mars and Venus.

We also assume that the extra cost at departure due to the Earth gravitational field is compensated at arrival at Mars, so the Earth and Mars gravitational potentials are not explicitly included here. Thus the motion of the spacecraft is given by the equations, that in the synodic reference frame and dimensionless units, are given by

$$\begin{aligned} \ddot{x} - 2\dot{y} &= \Omega_x, \\ \ddot{y} + 2\dot{x} &= \Omega_y, \end{aligned} \qquad [1]$$

where Ω is the effective potential given by

$$\Omega(x,y) = \frac{x^2+y^2}{2} + \frac{1-\mu}{r_1} + \frac{\mu}{r_2} + \frac{\mu(1-\mu)}{2}, \qquad [2]$$

with $r_1^2 = (x+\mu)^2 + y^2$ and $r_2^2 = (x-1+\mu)^2 + y^2$ being the square of the dimensionless distances from the spacecraft to the primaries P_1 and P_2, respectively, which are located at $(-\mu, 0)$ and $(1-\mu, 0)$. For the Sun-Jupiter system, μ, the normalized mass of P_2, equals 9.531609×10^{-4}.

This dynamical system has a first integral, called the Jacobi integral, given by

$$J(x,y,\dot{x},\dot{y}) = 2\Omega(x,y) - (\dot{x}^2 + \dot{y}^2) = C_J. \qquad [3]$$

2.1 Inclusion of Gravity assit by Venus

Gravity assist maneuver technique has been exploited in many space missions over the last decades. The hyperbolic encounter with the planet may be used to increase or decrease the absolute value and orientation of the velocity vector with respect to the Sun (or another third main body), as a spacecraft flyby a planet (or a general second body). In general, this maneuver provides a non-propulsive change of the heliocentric spacecraft energy which reduces the propellant mass needed for a interplanetary mission. In particular, powered and unpowered Venus gravity assist has been proposed in Earth-Mars transfers design for many authors [1, 8]. In this work, we investigate the role played by an unpowered close approach by Venus in Earth-Mars transfers built in the context of the Sun-Jupiter system. In particular, we use the periapsis altitude at Venus approach as a control parameter to seek convenient arrival states at Mars (mathematical descriptions of swing-by process may be found in many references [9, 10, 2, 11]).

3. Computation of Earth-Mars transfers

In this paper the analyses are performed considering three reference frames and five stages as described as follows. As a first step, initial conditions (ICs) are defined in the inertial heliocentric reference frame in physical units. Initial positions and velocities are given by the circular orbit of the Earth. Then four parameters are introduced, namely, the angle α_{SJ} between the Sun-Jupiter axis and the x-axis of the heliocentric inertial frame, the angular parameter θ of the circular orbit of the Earth around the Sun, and the magnitude Δv_E and phase ξ of the vector of velocity increment at Earth departure.

Then, each initial condition is transformed to the Sun-Jupiter barycentric rotating frame following the usual normalization of the R3BP model [12]. At this second stage of the procedure, time evolution is given by the equations of motion [1] of the Planar Circular R3BP for the Sun-Jupiter system.

When a trajectory eventually intersects the Sphere of Influence of Venus, a second transformation frame is performed to the inertial frame centered at Venus. In this stage, the dynamics is patched with the two-body temporal evolution with Venus as the main body. Besides that, at the boundary of the Venus's sphere of influence, maneuvers of negligible costs are responsible for producing variations of the periapsis altitude with respect to Venus. With that, a new parameter is included in the analysis and different trajectories are obtained. At the exit of the Venus's sphere of influence, for each trajectory, a new patching transformation between the Venus two-body reference frame and the Sun-Jupiter barycentric rotating frame is carried out. Again, the Sun-Jupiter R3BP prescribes the time evolution of each solution, until eventually the Mars circular orbit is reached or final time occurs. In a complete Earth-Mars transfer, the total cost Δv_T is given by the sum of the velocity increment Δv_E at Earth departure and the velocity variation Δv_M at Mars arrival (which is given by the difference of the velocity vector of the spacecraft and the velocity vector of Mars). The value of the Jacobi constant is changed at Venus Swing-by and at Mars arrival.

Trajectories are integrated by a variable step size Runge-Kutta-Fehlberg 7th-8th order solver [13] with relative error under 10^{-14} and absolute error under 10^{-15}.

For direct Earth-Mars transfers, the procedure is similar, except for the fact that one trajectory have to reach the orbit of Mars directly, and in this case, Venus plays no role.

4. Results for Both Earth-Mars Transfer Strategies

Using the procedure described in Section 3, each initial conditions set is obtained varying Δv_E and ξ, the magnitude and phase of the velocity increment at Earth departure, for each pair α_{SJ}, θ.

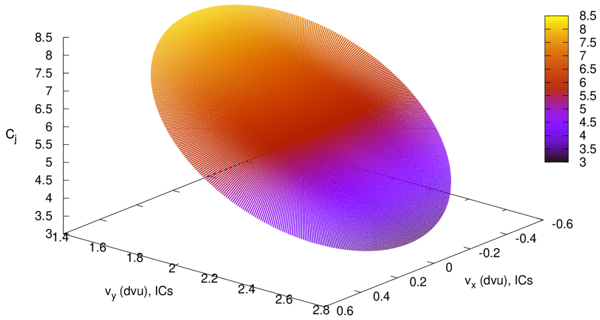

Figure 2: Jacobi constant versus the initial velocities expressed in the Sun-Jupiter d.v.u. for $\alpha_{SJ} = 0$ and $\theta = 0$.

In our numerical experiments, the range of values for Δv_E is from 0 to 10.0 km/s, with a fixed step of 0.02 or 0.05 km/s. Usually, 500 equispaced values of ξ are used, from 0 to 2π. As an illustration, Fig. 2 shows the Jacobi constant as a function of the Cartesian initial velocity values, expressed in the dimensionless velocity unit (d.v.u.) of the Sun-Jupiter system, for null values of α_{SJ} and θ.

As stated in Section 3, these ICs sets are integrated by Eqs. [1] with different goals according to two considered strategies. Namely, for direct transfers, trajectories must reach the Mars orbit, and for Venus swing-by, it is expected that the Venus sphere of influence is reached. However if these conditions are not fulfilled, time evolution is ended at the final time of 600 days. Results of each case are presented as follows.

4.1 Direct Earth-Mars Transfers

To verify the effect of Jupiter gravitational field in Direct Earth-Mars Transfers, we applied 16 equispaced values of α_{SJ}, from 0 to 2π, keeping $\theta = 0$ fixed. We mention that given the symmetries of the orbits, the θ value variation is not necessary.

Figure 3 shows the obtained results. The first frame (upper one) presents the Earth-Mars time of flight t_{EM} versus the total cost Δv_T for all obtained solutions (gray points), while Pareto solutions for minimum Δv_T are depicted by the black small circles and Hohmann transfer solution by the magenta star. We observe that the lowest cost solution is very similar to that of the Hohmann transfer, and that, as usual, solutions of lower transfer time are available for higher Δv_T values. The second frame presents the dependence of the lowest values of Δv_T with the integer index n_α, defined such that $\alpha_{SJ} = (n_\alpha - 1)\pi/8$. The color code represents the values of t_{EM} for these solutions. These results show that the effect of Jupiter is very tiny for Direct Transfers.

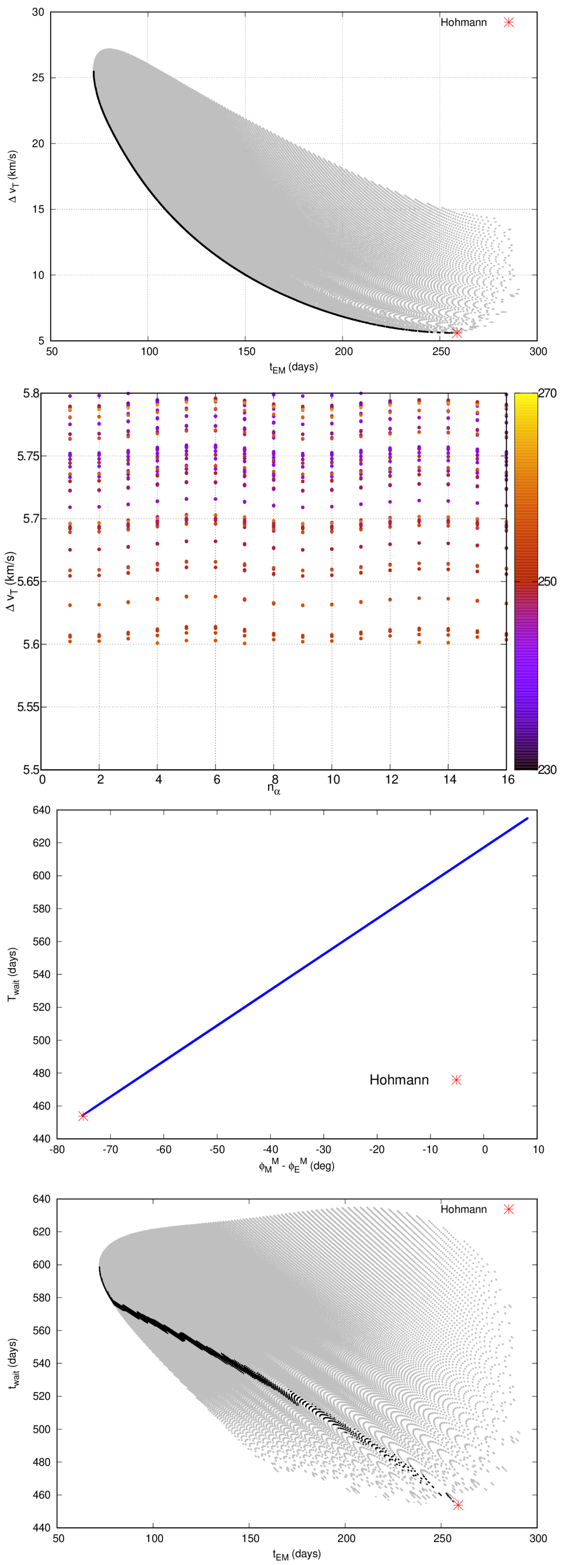

Figure 3: Results for Direct Earth-Mars Transfers for $\alpha_{SJ} = (n_\alpha - 1)\pi/8$, for $n_\alpha = 1, \cdots, 16$, and fixed null θ. Black circles on the top and bottom frames represent the Pareto solution for minimum values of Δv_T for each t_{EM} value. Hohmann transfer values are represented by the magenta star. See details on the text.

Besides that, for these initial conditions, the relative phase between Earth and Mars at the spacecraft arrival at Mars implies that the waiting time t_{wait} for a return via Hohmann transfer is longer than that of an usual Earth-Mars Hohmann transfer [14]. The third and fourth frames of Fig. 3 present the waiting time t_{wait} as a function of $\phi_M^M - \phi_E^M$, i.e., the difference of the phase of Mars and the phase of the Earth at Mars arrival, and the Earth-Mars flight time t_{EM}, respectively. In the bottom frame, the black points represent the Pareto solutions showed in the upper frame.

Given the features presented, these solutions are not of interest due to their immediate applications. However they are useful to be compared with the transfers built in the next section that involve flybys for two planets, therefore dual purpose transfers.

4.2 Earth-Mars Transfers with Venus Flyby

As a first inspection of the Venus flyby process, Fig. 4 shows the periapsis altitude index at the Venus approach as a function of the initial velocities at Earth departure, for both null values of α_{SJ} and θ. Here, we used 207 values for the periapsis distance r_p in the range from 1.1 to 3.1 Venus mean radius. Given that these values of r_p are equally spaced (except for the first fifteen values that are halved), the r_p step corresponds to 60.5 km (Venus mean radius is about 6051.8 km). In the $v_x - v_y$ plane, all the initial conditions used in this experiment are depicted by gray dots. This figure illustrates the percentage of the ICs that reach Mars after Venus flyby and that the full range of r_p can generate solutions that reach Mars after a Venus flyby.

Figure 5 shows various Earth-Mars transfers generated with one single initial condition at the Earth departure (blue square).

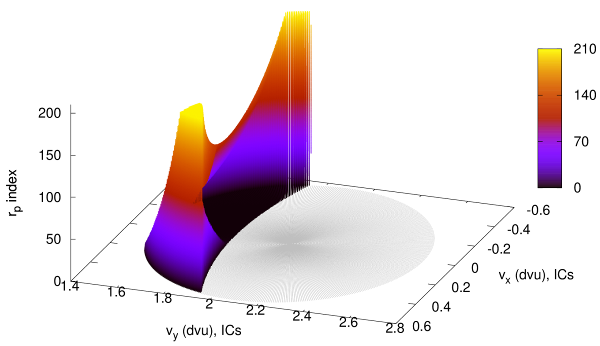

Figure 4: Periapsis altitude index at the Venus swing-by as a function of the initial velocities at Earth departure, for null values of α_{SJ} and θ. The gray dots at the horizontal plane show the full initial set for this pair of (α_{SJ}, θ).

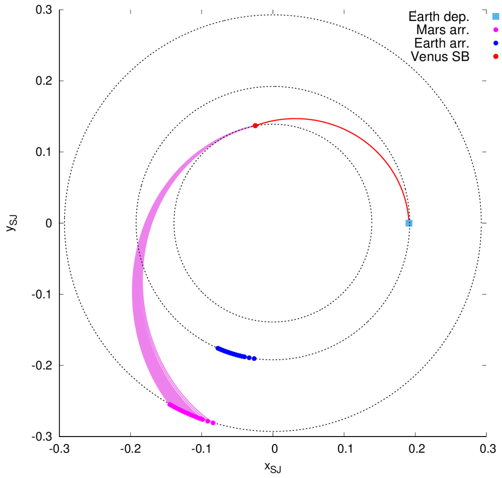

Figure 5: Illustration of the Venus swingby effect.

As time evolves, Venus sphere of influence is reached by the trajectory (red circle) and after the deflection with the Venus flyby for distinct periapsis altitude, various Venus-Mars trajectories are obtained (violet lines). In Fig. 5, the magenta points represent the position of Mars at the instant of the spacecraft arrival, while the correspondent position of Earth is marked by the blue circles. The variation of the heliocentric velocity between the input and the output of the Venus sphere of influence may be up to 8 km/s.

In order to inspect the effect of Jupiter in the Earth-Mars transfers with gravity assisty by Venus, a variation of α_{SJ} with a step of $\pi/8$ was performed (as before, each value of α_{SJ} is labeled by the integer n_α, from 1 to 16).

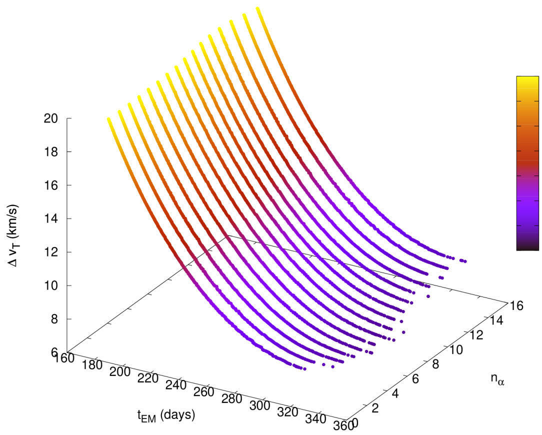

Figure 6: Optimal solutions for Earth-Mars transfers with Venus Flyby. Δv_T versus t_{EM} are shown for each value of n_α. The color code represents Δv_T.

Among the several obtained transfers, the solutions for minimum Δv_T are sought as a function of t_{EM}, for each value of n_α. Figure 6 presents the full Pareto front obtained for each initial phase α_{SJ}. The range obtained for t_{EM} is between 180 and 350 days, while the values of Δv_T varies from 7.378 up to 20 km/s.

A magnification of the lowest values of Δv_T as a function of n_α is presented in Fig. 7, at which the colors represents t_{EM} from 250 and 400 days.

Unlike for direct transfers, the Jupiter gravitational field plays an important role for transfers with Venus flyby, as highlighted by these results. For $\theta = 0$, the minimum value of Δv_T, 7.378 km/s, is found for n_α=7, i.e., $\alpha_{SJ} = 3\pi/4$, while the highest value of the minimum values (7.868 km/s) is found for n_α=1, i.e., α_{SJ}=0. This represents a variation of 0.490 km/s. Therefore, the judicious choice of the relative phase of Earth and Jupiter at the departure can lead to a significant fuel save of the mission. For the simplified model we employed and before a full optimization procedure, we found a save of 6.2 %.

For this optimal transfer, shown in Fig. 8 in the rotating frame of the Sun-Jupiter system, the time of flight between Earth and Venus is 132 days, while the Earth-Mars transfer takes 343 days. It requires Δv_E=2.60 km/s, Δv_M=4.478 km/s, while the Venus swing-by produces a variation of 4.83 km/s in the heliocentric inertial velocity. Also with respect to the heliocentric inertial frame, the phase of Venus when the spacecraft reaches its sphere of influence is 156.2°. At the spacecraft Mars arrival, the phases of the Earth and of Mars are respectively 338.2°and 327.6°. A waiting time of 594 days would be required for a return Hohmann transfer to the Earth.

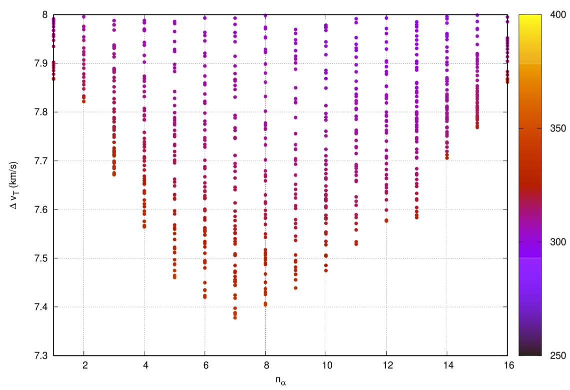

Figure 7: Magnification of the lowest values of Δv_T of the optimal solutions as a function of n_α. The color of the points are defined by t_{EM}.

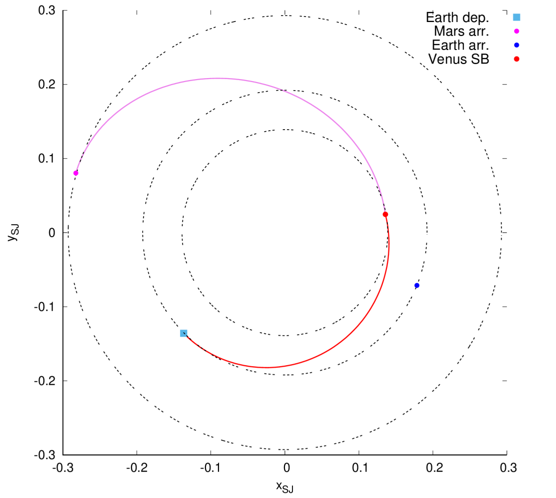

Figure 8: Optimal Earth-Mars transfer with Venus swing-by.

In general the waiting time of these Pareto transfers for a Hohmann return is between 573 and 685 days, which are very high. So alternative solutions must be sought for the return leg. However, if higher values of Δv_T are allowed, we find solutions for Hohmann return with waiting time from 0 to 24 days. These solutions are showed by Fig. 9.

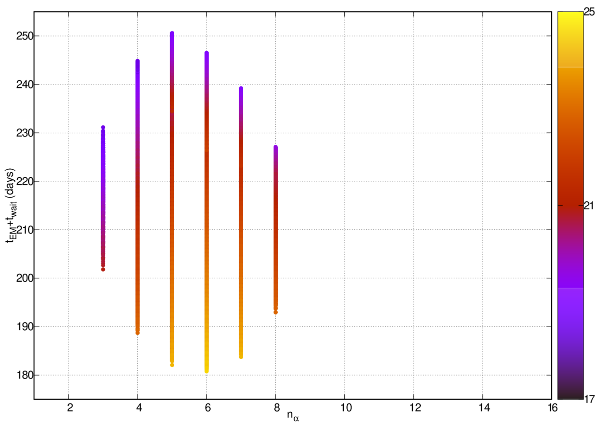

Figure 9: Transfer solutions with short waiting time for a Hohmann transfer return. The sum of t_{EM} and t_{wait} (in days) are shown for each α_{SJ}, while the colors depict the Δv_T (km/s).

5. Conclusions and Perspectives

In this paper, we obtained Earth-Mars transfers taking the gravitational effect of Jupiter and the Sun into account for solutions that performs a swing-by by Venus as well as for direct transfers. While gravitational effects of Jupiter are not relevant for direct transfers, the save of fuel for transfers with double visit, i.e., by Venus and Mars, may be significant. Furthermore, optimal solutions were obtained presenting the trade-off between total Δv and flight time between Earth and Mars.

In this perspective, many are the possible future analyses to be performed with different goals. First, multi-objective optimization strategy must be added in order to enable the inclusion of more realistic characteristics to the dynamical model, such as, the 3D orbits of Mars and Earth. Besides that, a impulsive thrust must be included at the swing-by by Venus at different points in the hyperbolic approach trajectory aiming to decrease the value of Δv_M or even to enable future purposes after Mars passage.

Acknowledgements

The authors thank to FAPESP (Brazil), grants 2016/24970-7, 2016/24561-0, and 2019/22678-5.

References

[1] S. Striepe and R. Braun, "Effects of a venus swingby periapsis burn during an earth-mars trajectory," *The Journal of the Astronautical Sciences*, vol. 39, pp. 299–312, 1991.

[2] A. Ferreira, A. Prado, and O. Winter, "A numerical study of powered swing-bys around the moon," *Advances in Space Research*, vol. 56, pp. 252–272, 2015.

[3] A. B. de Almeida Prado, *Optimal transfer and swing-by orbits in the two-and three-body problems*. PhD thesis, Department of Aerospace Engineering and Engineering Mechanics-University of Texas, 1993.

[4] Y. Ren, J. Masdemont, G. Gòmez, and E. Fantino, "Two mechanisms of natural transport in the solar system," *Communications in Nonlinear Science and Numerical Simulation*, vol. 17, pp. 844–853, 2012.

[5] G. Mingotti, F. Topputo, and F. Bernelli-Zazzera, "Earth-mars transfers with ballistic escape and low-thrust capture," *Celestial Mechanics and Dynamical Astronomy*, vol. 110, pp. 169–188, 2011.

[6] R. Eapen and R. Sharma, "Mars interplanetary trajectory design via lagrangian points," *Astrophysics and Space Science*, vol. 353, pp. 65–71, 2014.

[7] F. Topputo and E. Belbruno, "Earth-mars transfers with ballistic capture," *Celestial Mechanics and Dynamical Astronomy*, vol. 121, pp. 329–346, 2015.

[8] W. Hollister and P. J.E., "Optimum transfer to mars via venus." AIAA Paper No. 65-700, AIAA/ION Astrodynamics Specialist Conference, Monterey, CA, U.S.A.

[9] C. Brown, *Spacecraft Mission Design*. AIAA Education Series, 1998.

[10] J. Prussing and B. Conway, *Orbital Mechanics*. Oxford University Press, 2013.

[11] R. A. Broucke, "The celestial mechanics of gravity assist," in *Proceedings of AIAA/AAS Astrodynamics Conference, AIAA Paper 1988–4220*, 1988.

[12] P. Sousa-Silva, M. Terra, and M. Ceriotti, "Fast earth-moon transfers with ballistic capture," *Astrophysics and Space Science*, vol. 363, p. 210, 2018.
[13] J. Stoer and R. Bulirsch, *Introduction to Numerical Analysis*. Springer, 2002.
[14] H. Curtis, *Orbital Mechanics for Engineering Students*. Butterworth-Heinemann, 3 ed., 2014. Section 8.3.